P5.4 THE HYDROLOGICAL ONSET AND WITHDRAWAL INDEX (HOWI) FOR THE WEST AFRICA MONSOON

Giovanni A. Dalu, Marco Gaetani
Institute of Biometeorology - CNR, Rome, Italy
Francesco Meneguzzo, Alfonso Crisci, Giampiero Maracchi
Institute of Biometeorology - CNR, Florence, Italy
Francesca Guarnieri
Industrial Innovation Through Technological Transfer, University of Florence, Florence, Italy
Valerio Capecchi
Institute of Biometeorology - CNR, Florence, Italy

1. INTRODUCTION

Monsoons originate in the tropics to move poleward as they mature. They are driven by the summer ocean-continent temperature contrast, which causes a substantial change of direction of the large scale flow, driving the ocean moisture far inland and causing abundant seasonal rainfall. The South Asia-Australia monsoon is the largest of such systems. An exhaustive description of the tropical flows and of the monsoonal regimes has been done by Asnani (1993) and by Webster and coworkers (1987-1998).

The West Africa monsoon originates in the Gulf of Guinea, and moves northward feeding on the moisture advected from the tropical Atlantic. Mohr (2004) finds that there is a daily pulsation of the convective activity. We find a daily pulsation of the low tropospheric wind with a strong north-east polarization coarsely resolved in the NCAR/NCEP data (not shown). The rainfall has a long term trend and an intraseasonal variability, the years 1950-1970 were wetter than the years 1971-1990, with an additional intraseasonal variability at different time scales (Fig. 3 in Poccard et al, 2000; Fig. 1 in Le Barbè et al, 2002). A wavelet analysis shows a quasi-period at 5 day, at 15 day, and at 45 day (Fig. 1, in Janicot and Sultan, 2001). The synoptic scale pulsation, 5-7 day, is related to the easterly waves, which propagate eastward with a phase speed of 8-12 m/s with a wavelength of 3000-5000 km, carrying baroclinic instabilities (Diedhiou et al, 1999; Grist, 2002; Grist et al, 2002). Semazzi and Sun (1997) relate the intraseasonal variability to the fluctuation (position and intensity) of the high in the Libyan desert. Louvet et al (2003) shows that WAM establishes itself through active phases and pauses, which have a timescale of the order of the low seasonal variability observed by Janicot and Sultan (2001). While, the longer quasi-periodic intraseasonal variability of WAM may well have more remote connections (Knippers, 2003) as far as the West Pacific warm pool through the Madden-Julian oscillation (Matthews, 2004). Summarizing, WAM moves northward penetrating inland in pulses of different time scale, from 1 to 60 day.

The rainfall and the number of rain events per day show that the monsoon is bimodal in the Guinea region, with a single mode in the Sahel. In Cotenou (Gulf of Guinea), the rainfall has a main maximum in early summer and a minor maximum in late summer. In Parakou (South Sahel), it has a minor maximum in early summer and a main maximum in late summer. In Niamey (North Sahel), it has a single maximum (Fig. 7 and Fig. 8 in Le Barbè et al, 2002; Fig. 3 in Sultan and Janicot, 2000).

Sultan and Janicot (2000 - 2003) describe the dynamics of the West Africa monsoon, establishing two well distinct phases: the preonset and an onset phase. The preonset phase occurs in late spring, when the intertropical convergence zone (ITCZ) establishes itself at 5°N, climatologically at May 14. The actual onset, occurs when the ITCZ abruptly shifts northward, climatologically at June 24. The ITCZ moves from 5° to 10°N, where it stays for the whole month of August.

* *Corresponding author address:* Giovanni A. Dalu, Institute of Biometeorology - CNR, Rome, Italy; e-mail: g.dalu@ibimet.cnr.it

This is when the rainfall declines in the Guinea Gulf and increases in the South Sahel.

Using the NCEP/NCAR reanalysis (Kalnay et al, 1996) and the rainfall data of the Global Precipitation Climatology Project (Xie et al, 2003), we analyze the behaviour of the West African monsoon (WAM) between 10°W and 10°E (Sultan and Janicot, 2000 - 2003).

Table 1: WAM region and Sahel regions

	Longitude and latitude
WAM	10°E - 10°W and 5° - 20°N
Sahel	10°E - 10°W and 10° - 20°N
North Sahel	10°E - 10°W and 15° - 20°N

We focus on the subregions in Fig. 1 (Vizy and Cook, 2001 - 2002).

Table 2: Guinea and Sahel subregions

	Longitude and latitude
Guinea Gulf	10°E - 10°W and 0° - 5°N
Guinea Coast	10°E - 10°W and 5° - 10°N
South Sahel	10°E - 10°W and 10° - 15°N
North Sahel	10°E - 10°W and 15° - 20°N

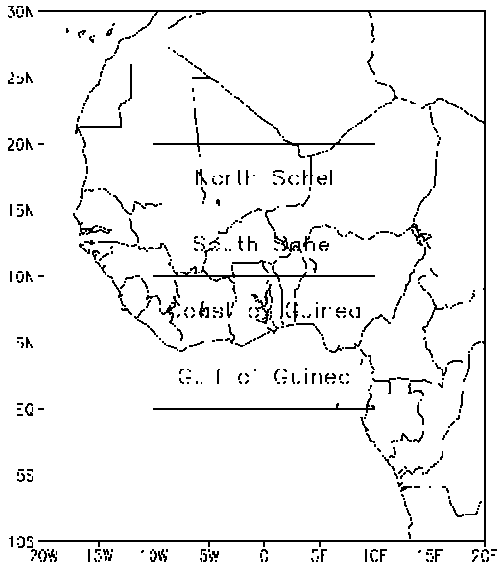

Figure 1: The West Africa monsoon regions in Table 2.

2. METHOD

In developing the HOWI for the West African monsoon, we limit our analysis to the period 1979-2002 in order to minimize variation of quality accuracy (Trenberth et al, 2001). Since the monsoonal indices are usually based on rainfall, we use the normalized rainfall as a benchmark for the HOWI. Using the rainfall pentad values, R, from Global Precipitation Climatology Project (GPCP) dataset, we define, for the regions in Tables (1) and (2),

$$R_N = \frac{< R >}{max(< \bar{R} >)} \quad \text{and} \quad \bar{R}_N = \frac{< \bar{R} >}{max(< \bar{R} >)}, \tag{1}$$

where R_N is the normalized rainfall and $\overline{R}_N$ is its climatological value; $\langle R \rangle$ is the rainfall averaged within a 2-D region (Fig. 1) and $\langle \overline{R} \rangle$ is its climatological value. Hereafter we will use the operator "< >" to indicate an average over a longitude-latitude box, the operator "[ ]" an average along the zonal direction and the operator "-" the climatological mean.

Using the NCEP/NCAR reanalysis (Kistler et al, 2001), we compute $\vec{v}_{VIW}$, the horizontal vector wind vertically integrated in the lower troposphere, the vertically integrated moisture transport VIMT vector, $\vec{v}_{VIMT}$, and its zonal and meridional components, u_{VIMT} and v_{VIMT},

$$\vec{v}_{VIW} = \int_{p_0}^{850mb} \vec{v}\, dp \quad \text{and} \quad \vec{v}_{VIMT} = \int_{p_0}^{850mb} (q\vec{v})\, dp, \tag{2}$$

$$\text{with} \quad u_{VIMT} = \int_{p_0}^{850mb} (q\,u)\, dp \quad \text{and} \quad v_{VIMT} = \int_{p_0}^{850mb} (q\,v)\, dp. \tag{3}$$

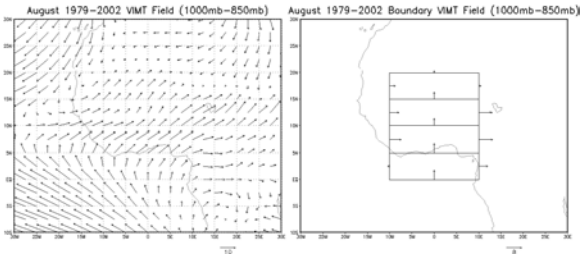

Figure 2: August climatology. a - Vertically integrated moisture transport, $\vec{v}_{VIMT}$. b - Zonal and meridional moisture inflow-outflow in the regions in Fig. 1 (Table 2).

The VIMT is restricted between the surface pressure p_0 and 850 hPa, since most of the moisture is confined within the first 1.5 km of the lower troposphere (see the vertical cross section of the specific humidity, q, in Fig. 3b). Because

of the structure of $\vec{v}_{VIMT}$ in Eq. (2), the VIMT vector is enhanced by the moisture and weakened by the dryness. The midsummer climatology of $\vec{v}_{VIMT}$ (month of August) shows where the moist south-westerly flow meets with the south-easterly dry flow, the 180° change in wind direction marks the northward limit of the monsoonal air, Fig. 2a. Since, in each subregion, the zonal moisture inflow balances the outflow (Fig. 2b), u_{VIMT} does not contribute to the onset and withdraw of WAM. Therefore, the HOWI is derived by the meridional component, v_{VIMT} ,

$$HOWI = 2\left\{\frac{< v_{VIMT} > - min(< \bar{v}_{VIMT} >)}{max(< \bar{v}_{VIMT} >) - min(< \bar{v}_{VIMT} >)}\right\} - 1. \qquad (4)$$

The onset of WAM occurs when HOWI ≥ 0, the withdrawal when HOWI ≤ 0. The HOWI ranges from -1 to +1, as the index developed by Fasullo and Webster (2003) for the Indian monsoon.

Since, within the region 10°W -10°E and 0° - 25°N, the meridional divergence is much larger than the zonal divergence (Fig. 4d), in this region the flow is almost 2-D. Therefore we can use a zonally averaged mass continuity equation:

$$\frac{\partial[v]\cos\theta}{r\cos\theta\partial\theta} + \frac{\partial[\omega]}{\partial p} = 0, \qquad (5)$$

where [*v*] is the meridional momentum component, zonally averaged between 10°W and 10°E; [ω] is the vertical velocity in pressure coordinates, θ is latitude, *p* is pressure, and *r* is the mean radius of the Earth. Using Eq. (5) we define the streamfunction Ψ,

$$\begin{cases} [v] = \frac{g}{2\pi r\cos\theta}\frac{\partial\Psi}{\partial p} \\ [\omega] = -\frac{g}{2\pi r^2\cos\theta}\frac{\partial\Psi}{\partial\theta}. \end{cases} \qquad (6)$$

The streamfunction is computed integrating vertically the 1st Eq. in (6) and enforcing $\Psi(p_{top} = 10hPa) = 0$ (Waliser et al, 1999),

$$\Psi = \frac{2\pi R\cos\theta}{g}\int_{p}^{p_{top}}([v] - [V])\,dp \quad \text{with} \quad [V] = \frac{1}{(1000 - p_{top})}\int_{1000}^{p_{top}}[v]\,dp. \qquad (7)$$

The mass-weighted vertical mean [*V*] is subtracted from [*v*] to prescribe no net mass flow across a meridian.

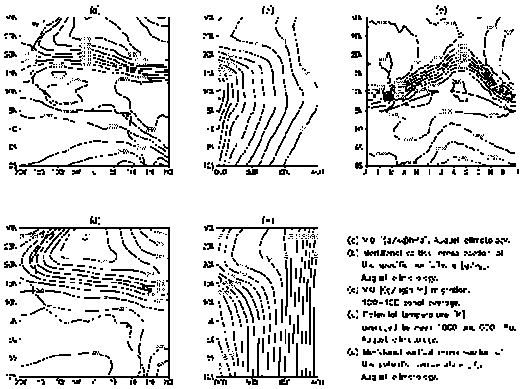

Figure 3: a - August climatology of the vertically integrated moisture, VIQ. b - August climatology of the meridional vertical cross section of the specific humidity, q. c - Meridional migration of [VIQ]. d - August climatology of the potential temperature, vertically averaged between 1000 and 600 hPa. e - August climatology of the meridional vertical cross section of the potential temperature.

The ITCZ is defined as the thermal equator, where the surface meridional wind is discontinuous and the vertical motion is upward (Asnani, 1993). However, since, in the tropics, the gradients are usually small, this definition can fail in catching the position of the maximum rainfall, associated with the deep convection of the ITCZ. Hoskins et al (1999) identifies the region of potential development of deep convection in the tropics, using the upward vertical velocity at 500 hPa. Since over West Africa, the vertical velocity at 500 hPa is still rather noisy, we evaluate the latitude of the ITCZ, θ_{ITCZ} , using the upward vertical velocity at 300 hPa, $\omega(300)\uparrow < 0$.

$$\theta_{ITCZ} = \frac{\int_{-10}^{15}(\theta\ [\omega(300)\uparrow])\,d\theta}{\int_{-10}^{15}([\omega(300)\uparrow])\,d\theta}, \qquad (8)$$

where Eq. (8) is as the ITCZ Eq. used by Waliser and Gautier (1993), where the highly reflective clouds (HRC) has been replaced by [$\omega(300)\uparrow$]. The HRC index is the number of days in a given month, when a single pixel was covered by organized deep convective systems.

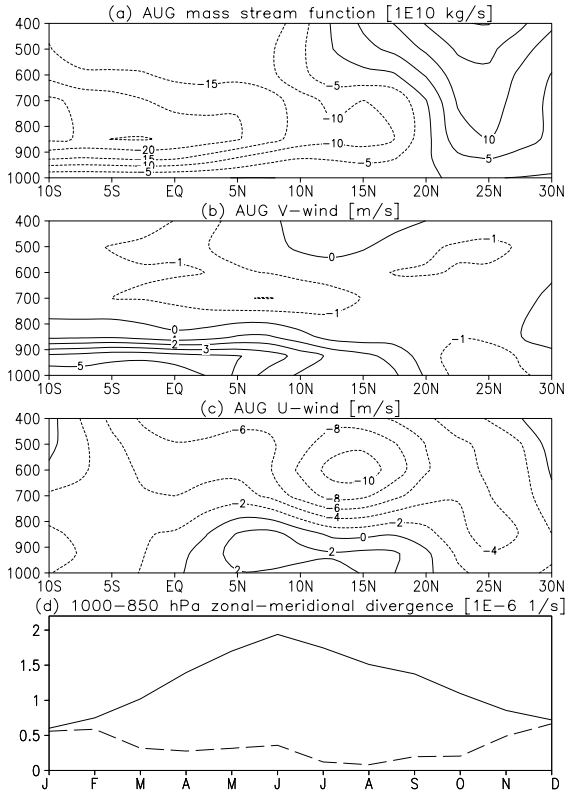

Figure 4: a - 2-D meridional streamfunction, Ψ, August climatology. b - Meridional vertical cross section of the meridional momentum component, August climatology. c - Meridional vertical cross section of the zonal momentum component, with the African easterly jet, EAJ, at 15°N and at 600 hPa, August climatology. d - Climatological meridional divergence (solid line) and zonal divergence (dashed line), within the region from 10°W to 10°E and from equator to 25°N. During the monsoon the mass flow is almost 2-D.

During the monsoonal season, the latitude, θ_q, of the maximum of the vertically integrated moisture VIQ, closely follows θ_{ITCZ}, see Fig. 3ac and Fig. 5ac.

$$\theta_q = \frac{\int_{2.5}^{12.5} (\theta\ [VIQ])\ d\theta}{\int_{2.5}^{12.5} ([VIQ])\ d\theta} \quad \text{with} \quad VIQ = \int_{p_0}^{850mb} q\,dp. \tag{9}$$

The intertropical front (ITF) is where the north-easterly dry wind, Harmattan, which has turned anticyclonically around the Libyan high, Fig. 8a, meets with the monsoonal moist south-westerly flow, Fig. 2a. The latitude of the ITF, θ_{ITF}, evaluated using $\omega(850)\uparrow$ < 0, migrates seasonally, staying about 1000 km further north of the ITCZ, see Fig. 5c and Fig. 5d.

$$\theta_{ITF} = \frac{\int_{10}^{22.5} (\theta\ [\omega(850)\uparrow])\ d\theta}{\int_{10}^{22.5} ([\omega(850)\uparrow])\ d\theta}. \tag{10}$$

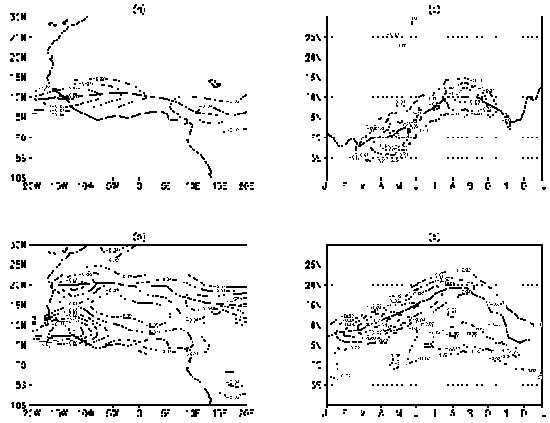

Figure 5: a - August climatology of the position of the ITCZ and $\omega(300)\uparrow$. b - August climatology of the position of the ITF and $\omega(850)\uparrow$. c - Meridional migration of ITCZ and $\omega(300)\uparrow$. d - Meridional migration of ITF and $\omega(850)\uparrow$.

The warmest air in the lower troposphere is between 20° and 25°N, Fig. 3e. This air is uplifted at the frontal edge by the moist cooler monsoonal air (20°N in August), and glides over it, Fig. 4a, generating the easterly low level jet, AEJ, halfway between the ITCZ and the ITF at the 600 hPa level (15°N in August, Fig. 4b).

3. DISCUSSION OF THE RESULTS

3.1 *The double monsoon*

There is a double monsoon in the Guinea region, with two rainy seasons, (Gu and Adler, 2004). In the Sahel region, there is a single rain season. In West Africa, the bulk of the rainfall is the ITCZ region, and the ITCZ transits twice through the Gulf of Guinea and through the Guinea Coast, once at the onset of WAM and a second time at the withdrawal. In fact that the ITCZ transits through the equator at the end of April, it moves northward till the end of July, it stays around 10°N through the month of August, then it moves back southward from September onward, Fig. 5c. Therefore, in the Gulf of Guinea, the rain season is longer, starts earlier

and finishes later than in the Guinea Coast, with a mid-summer relative minimum, more pronounced in the Gulf of Guinea. In midsummer, while the rainfall is at its relative minimum in the Guinea region, it reaches its maximum in the Sahel. In the South Sahel the rainfall maximum is larger and is reached earlier than the maximum in the North Sahel. The rainfall in the four regions defined in Table (2) is shown in Fig. 6b. It is worth to notice that the double monsoon is observed only at subregional scale, Fig. 6b, at regional scale the rainfall has always a single maximum, Fig. 6a.

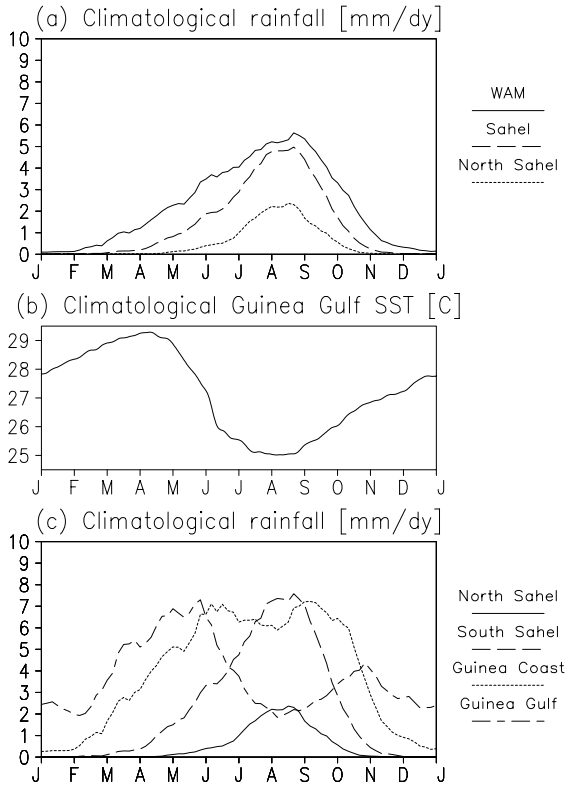

Figure 6: a - Climatology of the rainfall in mm/dy, pentad values runned through a 3-point filter, in the regions in Table (1), and c - in the regions in Table (2). b - Climatology of the SST [C] averaged in the Gulf of Guinea region, computed using the daily means from Reynolds SST dataset, 5-points filtered.

In the first half of the monsoonal season, the ITCZ moves northward and reaches its maximum northward position in August, Fig. 5ac. South of 10°N, i.e. in the in the Guinea Coast in the southern edge of the Sahel, the rain comes from the deep convection within the ITCZ region, Fig.5c. The primary source of moisture of the West Africa monsoon is the tropical Atlantic. The rainfall of the Guinea region follows the pattern of SST in the Gulf of Guinea: a SST maximum (April) precedes the first relative rainfall maximum in the Gulf of Guinea (May) and in the Coast of Guinea (June), the second relative rainfall maximum occurs in the Gulf (November) and in the Coast (September) when the SST begins to grow after the August minimum, Fig. 6bc. However, the moisture maximum in the lower troposphere closely follows the migration of the ITCZ (and the rainfall maximum), Fig.3c. Therefore there is a sizeable moisture contribution from re-evaporation of the rain in the ITCZ region to moisture of the Sahel region, 10°-20°N (Xue et al, 2004). The pressure gradient in the lower troposphere associated to the temperature distribution between 10° and 20°N drives the moist air into the Sahel region. The configuration is as a large seabreeze with hot dry air over the Sahara desert and cool monsoonal air moving northwards as a density current, Fig. 3e. The frontal edge of this density current (ITF) migrates northward, reaching its maximum northward position in August at 20°N, Fig. 5d. The moisture and the temperature fall gently between the ITCZ and the AEJ (10°-15°N), and then rapidly between AEJ and the ITF (15°-20°N), Fig. 3ac. The barotropic instability at the ITF, through pulsation, favours the intrusion of the moist air into the North Sahel region (15°-20°N). The baroclinic instability, associated to the AEJ halfway between the ITCZ and the ITF, at 600 hPa (Fig. 4b), triggers the moist convection in the Sahel region, lifting the moisture from the lower troposphere through the dry desert air. Rowell (2003) finds that the south-easterly flow from the eastern Mediterranean sea driven by the Libya high crosses the east Sahara desert, bringing a fair amount of moisture into the Sahel region, favouring the moist the convection. The horizontal temperature gradients are smaller in the South Sahel (less vertical shear and baroclinicity) than in the North Sahel, however, the specific humidity is sufficiently larger in the South Sahel, therefore the rainfall is more abundant in the South Sahel than the region between the AEJ and the ITF. For a more

throughful study on the barotropic-baroclinic instability in the Sahel region see Thorncroft and coworkers (1994a, b and 1999).

3.2 *The climatological HOWI*

In the regions in Table (1), the HOWI and the normalized rainfall, shows that the onset of monsoon is slower than the withdrawal, Fig. 7. The onset of the monsoon occurs when $\overline{R}_N$ exceeds 1/2, and the withdrawal when $\overline{R}_N$ falls below 1/2. The HOWI transition into positive values precedes the onset of 2-6 weeks, the HOWI return to negative values lags the withdrawal by less than a 1/2-1 week. The time lag between the preonset, determined using the HOWI, and the onset, determined using the climatological normalized rainfall, decreases with increasing latitude. The results are summarized in Table (3).

In each region in Table (1), the HOWI is a valuable predictor for the preonset of the monsoon, Fig. 7. The time given in Table (3) is in good agreement with the time given for the preonset, onset, and withdrawal by Sultan and Janicot (2000, 2003) and Janowiak and Xie (2003).

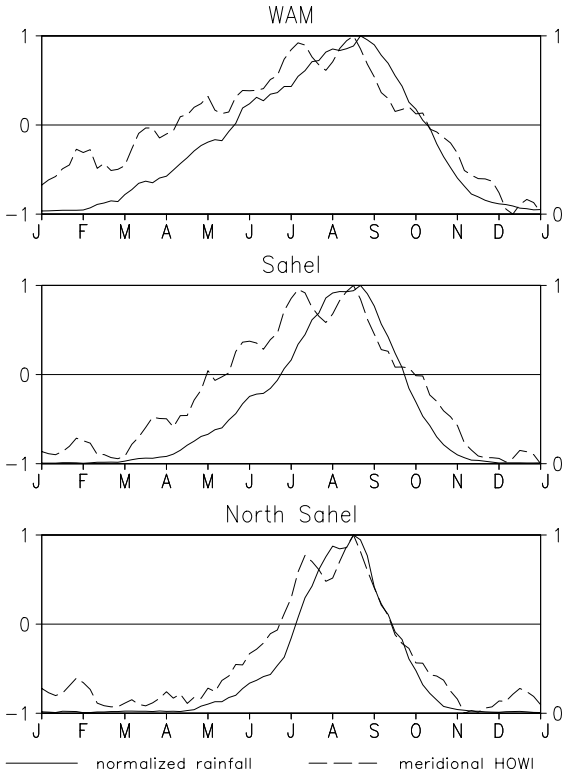

Figure 7: Climatology of the HOWI and normalized rainfall in the regions in Table (1), pentad values (3-point filtered).

Table 3: Climatology.

	HOWI onset, rain onset and rain withdrawal
WAM	APR 1st week | MAY 2nd week | OCT 2nd week
Sahel	APR 4th week | JUN 2nd week | SEP 4th week
North Sahel	JUN 2nd week | JUL 1st week | SEP 2nd week
	Lag between HOWI and rain at the onset and at the withdrawal
WAM	7 weeks | 0 weeks
Sahel	6 weeks | -0.5 weeks
North Sahel	2 weeks | 0 weeks

3.3 *Remote WAM connections*

According to Hoskins (1996) and Rodwell and Hoskins (1996), the Indian monsoon, through the Rossby waves, enhances the subsidence over the Sahara, while the West African monsoon enhances the high of the North Atlantic anticyclone. These are a 2-way interactions, since the Libyan anticyclone controls the north-east flow into WAM (Semazzi and Sun, 1997), while the North Atlantic anticyclone controls the north-west flow towards the Sahelian region. In Fig. 8 we show how the rainfall in the West African monsoon and in the Sahel relates to these features. Results shows that the North Atlantic anticyclone and the Indian monsoon low are positively correlated with the rainfall in the WAM region. The Libyan high is well correlated with rainfall in the Sahel only in the first half of the monsoonal season.

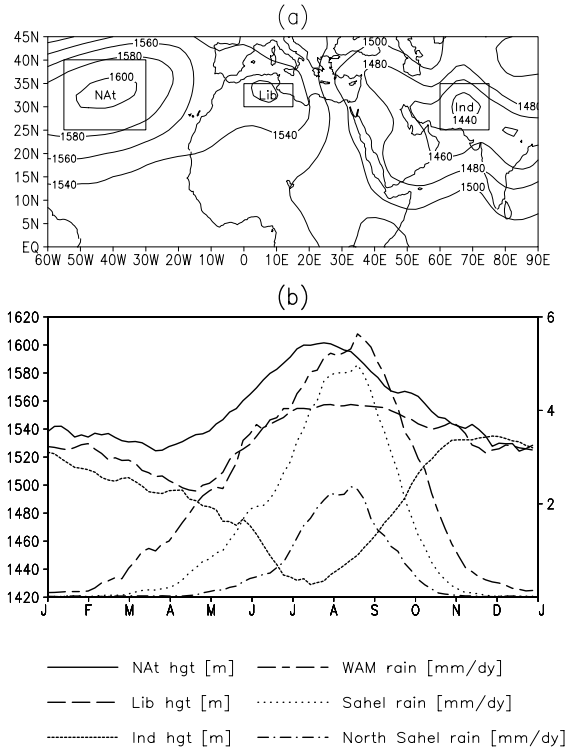

Figure 8: a - August climatology of the 850 hPa geopotential in the North Atlantic anticyclone, the Libyan desert, and the Indian monsoon. b - Climatology of the 850 hPa in the North Atlantic anticyclone, the Libyan anticyclone, the Indian monsoonal low and the rainfall in the regions in Table (1).

3.4 *The HOWI and R_N in 1998-2001*

In 1998 and 1999 the monsoon was strong, while, in 2000 and 2001, it was weak (Mohr, 2004). We compute the HOWI and normalized rainfall R_N for these years in the regions shown in Fig. 1, to compare how well the HOWI relates to the rainfall, in the WAM region, in the Sahel region, and in the North Sahel, Fig. 9. When, within the time lag between the HOWI and the rain onset, the HOWI falls back (decreases), we have "bogus" onset, Flatau et al (2003). Such bogus monsoon onsets are seen in 1998, 1999 in the Sahel and in the North Sahel in 2001.

3.5 *Additional WAM indicators: wind direction and SSTA in the Guinea Gulf*

When the monsoon reaches a region, there is a strong north-east polarization of the VIMT vector, $\vec{v}_{VIMT}$ (Fig. 2). Because of the structure of $\vec{v}_{VIMT}$ in Eq. (2), the north-easterly orientation of $\vec{v}_{VIW}$ can be used as a marker of the monsoon presence in that region, Fig.10. Results shows the presence of monsoonal rainfall whenever the zonal and the meridional wind components are both positive. The relation between positive zonal wind component and monsoon has already been noticed by Sultan and Janicot (2003).

The Guinea Gulf SSTA confirms the role of tropical Atlantic in moisture feeding into the WAM: the monsoon was stronger in 1998-1999 than in 2000-2001, when the summer SST was colder, Fig. 10d.

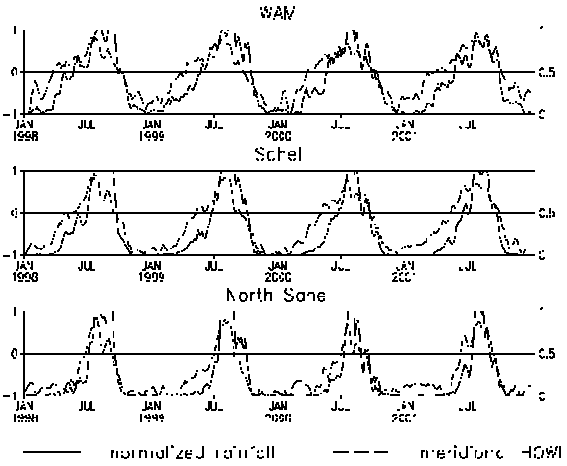

Figure 9: In 1998-1999 the rainfall was abundant, in 2000-2001 scarse. a - Normalized rainfall and HOWI in the WAM region, b - in the Sahel, and c - in the North Sahel (pentad values, 3-point filtered).

4. CONCLUSIONS

Using the NCEP/NCAR reanalysis and the GPCP the rainfall data, we analyze the behaviour of the West African monsoon in the region confined between 10°W – 10°E and 0° - 20°N. Results show that the ITCZ moves northward from its position at 3°N in spring to reach 10°N in August, where it stays for a month, and it retreats southward in early fall.

South of 10°N the rainfall is mainly due to the deep convection induced by the ITCZ. While in the Sahel (bounded by the ITCZ to the south

and by the ITF to the north, 10° - 20°N), the rainfall is induced by the combined action of barotropic-baroclinic instabilities (Thorncroft, 1994a, b; 1999).

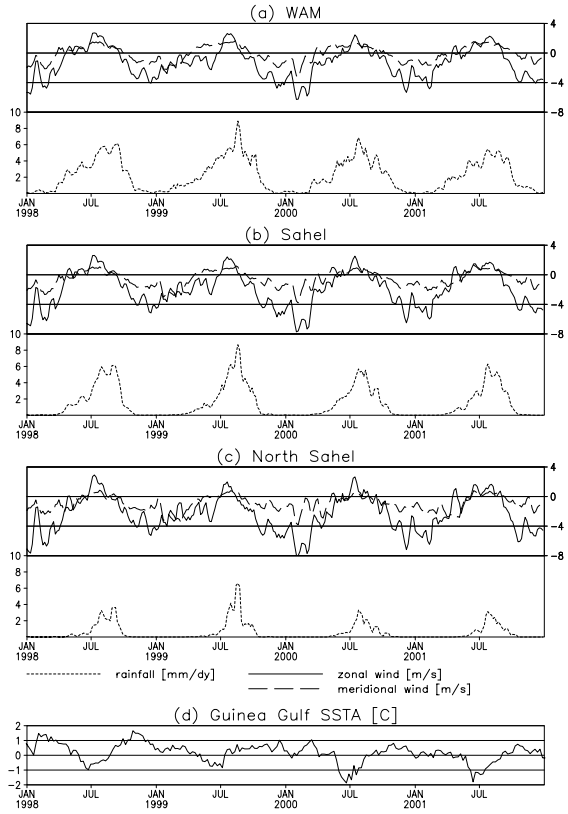

Figure 10: a, b, c - Zonal and meridional wind component in m/s ($u \sim 2v$), vertically averaged between 1000 and 850 hPa, and rainfall in mm/dy in the years1998-2001 (pentad values, 3-point filtered), in the regions in Table (1). d - Gulf of Guinea SSTA [C], weekly data from 1990 to present (Reynolds SST dataset).

We have analyzed the advection of moisture from the Gulf of Guinea into the West African monsoon region, and we find that part of the moisture advection in the Sahel comes from re-evaporation of the rain from the ITCZ region. The relative importance of the re-evaporation grows when the monsoon becomes mature, and the advection from the Guinea Gulf weakens.

We have developed a hydrological index for the onset and the withdrawal of WAM, HOWI, which is based on the meridional component of the VIMT, integrated up to 850 hPa (the HOWI is positive at the preonset of the monsoon, and it returns negative at its withdrawal). The HOWI precedes the half-value of the rainfall of 2-6 weeks, with the length of the pre-warning decreasing for increasing latitude. The withdrawal of WAM is more rapid than the onset with the HOWI returning negative at the half-value of the normalized rainfall. In addition, we show that the HOWI index has been shown valuable aid in recognizing bogus onsets in the infancy of WAM.

In the region interested by the monsoon, the wind in the lower troposphere is strongly polarized to north-easterly, with a distinct daily pulsation. Therefore, the change of the positive sign of the zonal and of the meridional wind component indicates that the monsoon is arrived.

The moisture advection into the WAM region is related to the SST in the Gulf of Guinea: the monsoon is strong when the water in the gulf is warmer than its climate summer temperature, while the monsoon is weak when the water in the gulf is colder.

REFERENCES

Asnani, G.C., 1993: Tropical meteorology. Indian Institute of Tropical Meteorology, Pashan, India, book in two volumes.

Charney, J. G., 1975: Dynamics of deserts and droughts in the Sahel. *Quart. J. Roy. Meteor. Soc.*, **101**, 193-202.

Dalu, G.A., M. Baldi, R.A. Pielke Sr., and G. Maracchi, 2004: Width and depth of mesoscale cells in a f-plane, two-layer, shallow, hydrostatic model. *J. Atmos. Sci.*, **submitted**.

Diedhiou, A., S. Janicot, A. Viltard, and P. de Felice, 1999: Easterly wave regimes and associated convection over West Africa and tropical Atlantic: results from NCEP/NCAR and ECMWF reanalysis. *Clim. Dyn.,* **15**, 795-822.

Fasullo, J., and P.J. Webster, 2003: A Hydrological Definition of Indian Monsoon Onset and Withdrawal. *J. Climate*, **16**, 3200-3211.

Flatau, M.K., P.J. Flatau, J. Schmidt, and G.N. Kiladis, 2003: Delayed onset of the 2002 Indian monsoon. *Geophys. Res. Lett.*, **30(14)**, 1768, doi: 10.1029/2003GL017434.

Gill, A.E., 1982: Atmosphere and ocean dynamics. Academic Press, New York, 662 pp.

Grist, J.P., 2002: Easterly waves over Africa, part I: The seasonal cycle and contrasts between wet and dry years. *Mon. Weat. Rev.*, **130**, 212-225.

Grist, J.P., and S.E. Nicholson, 2001: A study of the dynamic factors influencing the interannual variability of rainfall in the West African Sahel. *J. Climate,* **14**, 1337-1359.

Grist, J.P., S.E. Nicholson, and A.I. Barcilon, 2002: Easterly waves over Africa, part II: Observed and modelled contrasts between wet and dry years. *Mon. Weat. Rev.*, **130**, 212-225.

Gu, G., and R.F. Adler, 2004: Seasonal evolution and variability associated with the West African monsoon system. *J. Climate*, **17**, 3364-3377.

Hoskins, B., 1996: On the existence and strength of the summer subtropical anticyclones. *Bull. Am. Soc.*, **77**, 1287-1291.

Hoskins, B., R. Neale, M. Rodwell, and G. Yang, 1999: Aspects of the large-scale tropical atmospheric circulation. *Tellus*, **51 A-B**, 33-44.

Janicot, S., and B. Sultan, 2001: Intraseasonal modulation of the convection in the West African monsoon. *Geophys. Res. Lett.*, **28**, 523-526.

Janowiak, J. E., and P. Xie, 2003: A Global-Scale examination of Monsoon-Related Precipitation. *J. Climate*, **16**, 4121-4133.

Kalnay, E., M. Kanamitsu, R. Kistler, W. Collins, D. Deaven, L. Gandin, M. Iredell, G. White, J. Woolen, Y. Zhu, M. Chelliah, W. Ebisuzaki, W. Higgins, J. Janowiak, K. Mo, and D. Joseph, 1996: NCEP/NCAR 40-year reanalysis project. *Bull. Am. Soc.*, **77**, 437-471.

Kistler, R.E., and coauthors, 2001: The NCEP-NCAR 50-Year Reanalysis: Monthly Means CD-ROM and Documentation. *Bull. Am. Met. Soc.*, **82**, 247-268.

Knippers, P., 2003: Tropical-extratropical interactions causing precipitation in Northwest Africa: Statistical analysis and seasonal variations. *Mon. Weat. Rev.,* **131**, 3069-3076.

Le Barbè, L., T. Lebel, and D. Tapsoba, 2002: Rainfall variability in West Africa during the Years 1950-90. *J. Climate*, **15**, 187-202.

Louvet, S., B. Fontaine, and P. Roucou, 2003: Active phases and pauses during the installation of the West Africa monsoon through 5-day CMAP rainfall data (1979-2001). *Geophys. Res. Lett.*, **30 No. 24**, 2271.

Matthews, A.J., 2004: Intraseasonal variability over tropical Africa during northern summer. *J. Climate*, **17**, 2427-2440.

Mohr, K.I., 2004: Interannual, monthly, and regional variability in the wet diurnal cycle of precipitation in the Sub-Saharan Africa. *J. Climate*, **17**, 2441-2453.

Otterman, J., 1974: Bring high-albedo soils by overgrazing: an hypothesized desertification mechanism. *Science*, **186**, 426-427.

Poccard, I., S. Janicot, and P. Camberlin, 2000: Comparison of rainfall structures between NCEP/NCAR reanalysis and observed data over tropical Africa. *Clim. Dyn.*, **16**, 897-915.

Qian, W., Y. Deng, Y. Zhu, and W. Dong, 2002: Demarcating the worldwide monsoon. *Theor. Appl. Climatol.*, **71**, 1-16.

Rodwell, M.J., and B.J. Hoskins, 1996: Monsoons and the dynamics of the deserts. *Quart. J. Roy. Meteor. Soc.*, **122**, 1385-1404.

Rodwell, M.J., and B.J. Hoskins, 2001: Subtropical anticyclones and summer monsoons. *J. Climate*, **14**, 3192-3211.

Rowell, D.P., 2003: The impact of the Mediterranean SSTs on the Sahelian rainfall season. *J. Climate*, **16**, 849-862.

Semazzi, F.H.M., and L. Sun, 1997: The role of orography in determining the Sahelian climate. *Int. J. Climatol.* **17**, 581-596.

Sultan, B., and S. Janicot, 2000: Abrupt shift of the ITCZ over West Africa and intra-seasonal variability. *Geophys. Res. Lett.*, **27**, 3353-3356.

Sultan, B., S. Janicot, and A. Diedhiou, 2003: The West African Monsoon Dynamics. Part I: Documentation of Intraseasonal Variability. *J. Climate*, **16**, 3389-3406.

Sultan, B., and S. Janicot, 2003: The West African Monsoon Dynamics. Part II: The "Preonset" and "Onset" of the Summer Monsoon. *J. Climate*, **16**, 3407-3427.

Thorncroft, C.D., and B.J. Hoskins, 1994a: An idealized study of the African easterly waves, Part I, a linear view. *Quart. J. Roy. Meteor. Soc.* **120**, 953-982.

Thorncroft, C.D., and B.J. Hoskins, 1994b: An idealized study of the African easterly waves, Part II, a nonlinear view. *Quart. J. Roy. Meteor. Soc.,* **120**, 983-1915.

Thorncroft, C.D., and M. Blackburn, 1999: Maintenance of the African easterly jet. *Quart. J. Roy. Meteor. Soc.*, **125**, 763-786.

Trenberth, K.E., D.P. Stepaniak, J.W. Hurrell, and M. Fiorino, 2001: Quality of the reanalysis in the tropics. *Clim. Dyn.*, **14**, 1499-1510.

Vizy, E.K., and K.H. Cook, 2001: Mechanisms by which Gulf of Guinea and eastern north Atlantic sea surface temperature anomalies can influence African rainfall. *J Climate*, **14**, 795-821.

Vizy, E.K., and K.H. Cook, 2002: Development and application of a mesoscale climate model for the tropics: Influence of the sea surface temperature anomalies on the West African monsoon. *J. Geophys. Res.*, **107, ACL 2**, 1-22.

Waliser, D.E., and C. Gautier, 1993: A satellite-derived climatology of the ITCZ. *J. Climate,* **6**, 2162-2174.

Waliser, D.E., Z. Shi, J.R. Lanzante, and A.H. Oort, 1999: The Hadley circulation: assessing NCEP/NCAR reanalysis and sparse in-situ estimates. *Clim. Dyn.*, **15**, 719-735.

Webster, P.J., 1987: The elementary monsoon. Monsoons, Wiley Interscience, pp 1-36.

Webster, P.J., 1994: The role of hydrological processes in the ocean-atmosphere interactions. *Review of Geophysics*, **32**, 427-476.

Webster, P.J., V.O. Magana, T.N. Palmer, J. Shukla, R.A. Tomas, M. Yanai, and T. Yasunari, 1998: Monsoons: Processes, predictability, and prospects for prediction. *J. Geophys. Res.*, **103 (Toga special issue)**, 14451-14510.

Webster, P.J., C. Clark, G. Cherikova, J. Fasullo, W. Han, J. Loschnigg, and K. Shami, 2002: The Monsoon as a self-regulating coupled ocean-atmosphere system. Meteorology at Millennium, Academic Press, 198-219.

Xie, P., J.E. Janowiak, P.A. Arkin, R. Adler, A. Gruber, R. Ferraro, R., G.J. Huffman, and S. Curtis, 2003: GPCP pentad precipitation analyses: an experimental dataset based on gauge observations and satellite estimates. *J. Climate*, **16**, 2197-2214.

Xue, Y., H. Juang, W. Li, S. Prince, R. De Friers, and Y. Jiao, 2004: Role of the land surface processes in monsoon development: East Asia and West Africa. *J. Geophys. Res.*, **109**, D03105, doi: 10.1029/2003JD003556.